Co-evolving wing spots and mating displays are genetically separable traits in *Drosophila*

Jonathan H. Massey[1,2], Gavin R. Rice[3], Anggun Firdaus[4], Chi-Yang Chen[4], Shu-Dan Yeh[4], David L. Stern[2]*, Patricia J. Wittkopp[1,5]*

[1]Department of Ecology and Evolutionary Biology, University of Michigan, Ann Arbor, MI, USA

[2]Janelia Research Campus, Howard Hughes Medical Institute, Ashburn, VA, USA

[3]Department of Biological Sciences, University of Pittsburgh, Pittsburgh, Pennsylvania, USA 15260

[4]Department of Life Sciences, National Central University, Taoyuan, Taiwan

[5] Department of Molecular, Cellular, and Developmental Biology, University of Michigan, Ann Arbor, MI, USA

*Corresponding authors

wittkopp@umich.edu; sternd@janelia.hhmi.org

Keywords: *Drosophila,* correlated traits, pigmentation, courtship behavior, *optomotor-blind*

Abstract

The evolution of sexual traits often involves correlated changes in morphology and behavior. For example, in Drosophila, divergent mating displays are often accompanied by divergent pigment patterns. To better understand how such traits co-evolve, we investigated the genetic basis of correlated divergence in wing pigmentation and mating display between the sibling species *Drosophila elegans* and *D. gunungcola*. *Drosophila elegans* males have an area of black pigment on their wings known as a wing spot and appear to display this spot to females by extending their wings laterally during courtship. By contrast, *D. gunungcola* lacks both of these traits. Using Multiplexed Shotgun Genotyping (MSG), we identified a ~440 kb region on the X chromosome that behaves like a genetic switch controlling the presence or absence of male-specific wing spots. This region includes the candidate gene *optomotor-blind* (*omb*), which plays a critical role in patterning the *Drosophila* wing. The genetic basis of divergent wing display is more complex, with at least two loci on the X chromosome and two loci on autosomes contributing to its evolution. Introgressing the X-linked region affecting wing spot development from *D. gunungcola* into *D. elegans* reduced pigmentation in the wing spots but did not affect the wing display, indicating that these are genetically separable traits. Consistent with this observation, broader sampling of wild *D. gunungcola* populations confirmed the wing spot and wing display are evolving independently: some *D. gunungcola* males preformed wing displays similar to *D. elegans* despite lacking wing spots. These data suggest that correlated selection pressures rather than physical linkage or pleiotropy are responsible for the coevolution of these morphological

and behavioral traits. They also suggest that the change in morphology evolved prior to the change in behavior.

Introduction

Animals often use colorful morphological structures to communicate with prospective mates during courtship (McKinnon and Pierotti, 2010). In vertebrates and invertebrates, pigmented bodies or wings often evolve together with specific components of courtship behavior that animals use to display their colorful anatomy (Loxton, 1979; Endler, 1991; Sinervo et al., 2000; White et al., 2015). These correlated differences evolve both within and between populations, frequently distinguishing males from females or closely related species (Gray and McKinnon, 2007; McKinnon and Pierotti, 2010). In the handful of case studies examining the genetic basis of such co-evolving traits, linkage mapping and genome-wide association studies (GWAS) have shown that loci affecting pigmentation patterning tend to co-localize with loci affecting variation in mating behaviors (Lindholm and Breden, 2002; Kronforst *et al*., 2006; Yeh *et al.*, 2006; Thomas *et al*., 2008; Kupper *et al*., 2016; Lamichhaney *et al*., 2016; Merrill *et al*., 2019; reviewed in McKinnon and Pierotti, 2010). That is, physical linkage of genetic variants underlies phenotypic correlations between mating behavior and pigmentation. Interestingly, these loci also tend to explain much of the variation observed for both traits (e.g., Kronforst *et al*., 2006; Kupper *et al*., 2016; Lamichhaney *et al*., 2016). A key challenge is determining how frequently these patterns of genomic architecture underlie correlated evolution and whether a single pleiotropic locus or separate linked loci are involved.

Disentangling whether pleiotropic or physically linked loci underlie patterns of correlated evolution between pigmentation and mating behavior is important for understanding how natural selection generates differences between sexes and species. If two beneficial traits are genetically correlated due to separate, physically linked loci, theory predicts that natural or sexual selection (e.g., through predation or female choice) will act to minimize recombination between the causal loci (Charlesworth and Charlesworth, 1976). It has been hypothesized that one solution to this problem might involve the evolution of chromosomal inversions that suppress recombination between two or more linked loci (Kirkpatrick and Barton, 2006). Alternatively, mutations at a single pleiotropic gene could cause correlated components of pigmentation and mating behavior to evolve simultaneously, although it is not likely, mechanistically, that a single mutation with generate adaptive changes in both pigmentation and behavior. Distinguishing between these genetic modes of phenotypic evolution requires, in part, high-resolution mapping of correlated traits.

In the Oriental *Drosophila melanogaster* species group, male-specific wing spots are phylogenetically correlated with mating displays (Kopp and True, 2002; Figure 1A). Species with wing spots perform elaborate wing display dances during courtship, extending their wings laterally, turning their dorsal wing surfaces toward the female, and waving them up and down; species without wing spots lack display behavior (Kopp and True, 2002, Figure 1A,B). Correlated gains and losses of both traits have evolved repeatedly (Kopp and True, 2002, Figure 1A). For example, in *D. elegans* and *D. gunungcola*, sibling species from this group that are estimated to have diverged 2-2.8 million years ago (Prud'homme *et al*., 2006), *D. elegans* (Bock and Wheeler, 1972) males possess wing spots and perform wing displays, whereas *D.*

gunungcola (Sultana *et al*., 1999) males lack both traits (Kopp and True, 2002; Prud'homme *et al*., 2006; Yeh *et al*., 2006; Figure 1B; Video 1; Video 2). Previously, Yeh *et al*., (2006) and Yeh and True (2014) discovered that *D. elegans* and *D. gunungcola* can generate fertile F_1 hybrid female offspring in the lab and they performed interspecific crosses to study the genetic basis of wing spot and wing display divergence. Through quantitative trait locus (QTL) mapping, they showed that evolution of linked loci on the X chromosome contributed to divergence in both traits (Yeh *et al.*, 2006; Yeh and True, 2014). One QTL explaining wing spot size variation was linked to the pigmentation gene *yellow*, supporting the hypothesis that *yellow cis*-regulatory divergence contributes to wing pigmentation evolution (Wittkopp *et al*., 2002a; Gompel *el al*., 2005; Prud'homme *et al*., 2006). It remained unclear, however, whether the same or different loci on the X chromosome underlie correlated differences in wing spot and wing display between these species.

To distinguish between these possibilities, we re-examined the genetic basis of wing spots and wing display divergence between *D. elegans* and *D. gunungcola.* Specifically, we (1) generated recombinant backcross progeny segregating for both traits, (2) assembled chromosome-length scaffolds of *D. elegans,* (3) used Multiplexed Shotgun Genotyping (MSG) (Andolfatto *et al*., 2011) to estimate recombination crossover positions across the genome, (4) generated quantitative measures of both wing spots and wing display behavior to estimate the effect size of loci contributing to divergence, and (5) generated advanced, recombinant introgressions on the X chromosome in an attempt to separate quantitative trait loci (QTL) underlying wing spots and wing display behavior. These experiments showed that a single locus on the X chromosome behaves like a genetic switch for wing spot divergence; however spotless males inheriting

introgressions of this region from *D. gunungcola* in a *D. elegans* genetic background performed wing displays like *D. elegans* males, indicating that the two traits are genetically separable. These findings suggest that wing spot and wing display behavior might have originally diverged independently. Consistent with this hypothesis, newly collected *D. gunungcola* strains from Indonesia appear to completely lack wing spots but retain the ability to perform wing displays. This observation suggests that the loss of wing spots occurred prior to the loss of wing display in the reference strain of *D. gunungcola* used in this study and in prior work.

Materials and Methods

Fly stocks

The *D. elegans HK* (Hong Kong) and *D. gunungcola SK* (Sukarami) lines used in this study were a gift from John True (Stony Brook University). Species stocks were kept on a 12 h light-dark cycle at 23ºC on a University of Michigan "R food" diet containing molasses (http://lab-express.com/flyfoodsupplies.htm#rfood) (Wirtz and Semey, 1982). Maintaining these species on R food at high densities (50-100 flies per vial) allowed for the parental population to build up to thousands of flies to collect hundreds of virgins for interspecific crosses (see below). Neither *D. elegans* nor *D. gunungcola* pupate on the sides of the vial, so adults were flipped out when 3rd instar L3 larvae developed and Fisherbrand filter paper (cat# 09-790-2A) was added to the food to create pupation space.

Generating hybrid progeny

Virgin males and females of *D. elegans* and *D. gunungcola* were isolated upon eclosion and stored in groups of ten for one week on University of Michigan "M food", which is the standard cornmeal diet from the Bloomington Drosophila Stock Center (https://bdsc.indiana.edu/information/recipes/bloomfood.html) with 20% higher agar content. Virgin males from *D. elegans* were crossed to virgin females from *D. gunungcola*, and virgin males from *D. gunungcola* were crossed to virgin females from *D. elegans* in groups of ten males and ten females to generate fertile F_1 female and sterile F_1 male hybrids. These crosses took ~3-4 weeks to produce hybrid progeny. The switch from R food to M food for interspecific crosses was necessary, because R food tended to accumulate condensation and bacterial growth much faster than M food when few flies occupied a vial. Since crossing *D. elegans* and *D. gunungcola* to generate F_1 hybrids tends to take several more weeks than within species crosses, the switch to M food diet allowed for maximum breeding time and the development of dozens of hybrid progeny. Once hybrid females eclosed from both interspecific cross directions, they were pooled into the same vial and aged for ten days. We did not keep track of F_1 hybrid female maternity, because previous work (Yeh and True, 2014) found no effect of F_1 hybrid maternity on trait means for wing spots and wing display in backcross populations. Multiple high-density groups of ~60 F_1 hybrid females were then backcrossed to ~60 virgin male *D. elegans* flies in individual vials on M food diet to create the *D. elegans* backcross recombinant population (724 individuals). To create the *D. gunungcola* backcross recombinant population (241 individuals), groups of ~60 F_1 hybrid females were backcrossed to ~60 virgin male *D. gunungcola* flies in individual vials on M food diet; this backcross was less successful at producing recombinant progeny than the *D. elegans* backcross direction.

158 *Behavioral assays*

159

160 Virgin *D. elegans* females were isolated upon eclosion, aged 10-20 days, and stored in groups of
161 30-40 for courtship assays. F_1 hybrid and recombinant backcross males were isolated
162 individually in M food vials using CO_2 upon eclosion for at least 5 days before each courtship
163 assay. For each assay, a single individual male was gently aspirated into a custom built 70 mm
164 diameter bowl arena that matches the specifications in Simon and Dickinson (2010). Next, a
165 single virgin *D. elegans* female was aspirated into the chamber and videotaped for the next 20
166 min, using a Canon VIXIA HF R500 camcorder mounted to Manfrotto (MKCOMPACTACN-
167 BK) aluminum tripods. Videos were recorded between 09:00 and 16:00 at 23ºC. *D. elegans*
168 virgin females were used in all courtship assays in case any *D. elegans* female cues were
169 necessary to elicit male wing display behavior. After each assay, both the male and female were
170 aspirated back into an M food vial and left for up to 5 days, after which each male was frozen in
171 individual 1.5 mL Eppendorf tubes for wing spot quantification (see Quantification of wing
172 spots), genomic DNA (gDNA) extraction, and sequencing (see Library preparation and
173 sequencing). All courtship videos (~900 total) are available here:
174 https://deepblue.lib.umich.edu/data/concern/data_sets/j098zb17n?locale=en.

175

176 *Quantification of wing display behavior*

177

178 F_1 hybrid and recombinant males from both backcross directions performed variable wing
179 display behaviors during courtship as described previously (Yeh *et al.*, 2006; Yeh and True,
180 2014). To generate quantitative measurements of wing display variation between individuals,

each courtship video was played using QuickTime (version 10.4) (Apple Inc., Cupertino, CA) software in a MacOS environment and digital screenshots were manually taken for each wing display bout, defined as a bilateral wing extension performed near the female (Supplementary Figure S1). Next, for each individual fly, wing display screenshots were compared to each other to identify the maximum wing display bout per fly, defined by comparing the distance between the tips of each wing relative to the center of the fly. These maximum wing display screenshots were then imported into ImageJ software (version 1.50i) (Wayne Rasband, National Institutes of Health, USA; http://rsbweb.nih.gov/ij/) to manually measure the "Maximum wing display angle" for F_1 hybrid and recombinant males. In ImageJ, each screenshot image was inverted using the "Find Edges" function to enhance the contrast between the arena background and the edges of the fly wings (Supplementary Figure S1). Next, the "Polygon Selections" tool was used to fit an ellipse around the fly body using the "Fit Ellipse" function (Supplementary Figure S1). A Macros function (Supplementary File S1) was then used to generate major and minor axes inside the ellipse to identify the center of the fly body (Supplementary Figure S1). Finally, the "Angle Tool" was used to measure the "Maximum wing display angle" centering the vertex at the intersection of the major and minor axes and extended from wing tip to wing tip (Supplementary Figure S1). "Maximum wing display angle" varied between ~50º and ~220º between backcross recombinant individuals.

Quantification of wing spots

Since wing spots fully form ~24 h after eclosion in *D. elegans*, all parental male *D. elegans*, *D. gunungcola*, F_1 hybrids, and backcross recombinants were aged at least 7 days before being

frozen at -20C in 1.5 mL Eppendorf tubes. Next, using a 20 Gauge stainless steel syringe tip (Techcon) (cat# TE720100PK) the right wing of each fly was cut away from the thorax and placed on a glass microscope slide (Fisherbrand) (cat# 12-550-15) to image using either a Leica MZFLIII stereoscope equipped with a Leica DC480 microscope camera or a Canon EOS Rebel T6 camera equipped with a Canon MP-E 65 mm macro lens. Each camera was calibrated using an OMAX 0.1 mm slide micrometer to define pixel density in ImageJ software. JPEG images of wings were imported into ImageJ to measure wing spot size relative to total wing area (wing spot size / total wing area). Total wing area (wing length x wing width) was approximated using length and width proxies following methods described in Yeh and True (2014). Using the "Polygon Selections" tool, the margins of black pigmentation defining each "Wing spot size" was traced and the polygon area quantified in mm^2 using the "Measure" function. "Wing spot size" varied between 0 mm^2 (spotless) and 0.15 mm^2 between recombinant individuals.

Library preparation and sequencing

We estimated chromosome ancestry "genotypes" for 724 *D. elegans* backcross progeny and 241 *D. gunungcola* backcross progeny with a single Multiplexed Shotgun Genotyping (MSG) (Andolfatto *et al*., 2011) library using 965 barcoded adaptors following methods described in Cande *et al*., (2012). In brief, to extract gDNA from all male backcross individuals, single flies were placed into individual wells of 96-well (Corning, cat# 3879) plates containing a single steel grinding bead in each well (Qiagen, cat# 69989). Eleven plates in total were prepared for 965 individual gDNA extractions. gDNA was isolated and purified using the solid tissue extraction procedure from a Quick-DNA 96 Kit (Zymo, cat# D3012) and a paint shaker to homogenize

227 tissue. gDNA was tagmented using a hyperactive version of Tn5 transposase charged with
228 annealed adaptor oligos following the methods described in Picelli *et al*. (2014). Unique
229 barcoded adaptor sequences were ligated to each sample of tagmented gDNA with 14 cycles of
230 PCR using OneTaq 2x Master Mix (NEB, cat# M0482S), and all samples were pooled into a
231 single multiplexed sequencing library. Agencourt AMPure XP beads (Beckman Coulter, cat#
232 A63881) were used to size select ~150-800 bp fragments and eluted in 35 uL of molecular grade
233 water (Corning, cat# MT46000CI). The library was quantified by qPCR and sequenced in a
234 single lane of Illumina HiSeq by the Janelia Quantitative Genomics Team.
235
236 In addition to generating the backcross sequencing library, both *D. elegans HK* and *D.*
237 *gunungcola SK* parental species were sequenced at 20x coverage using an Illumina MiSeq
238 Reagent Kit (v.3, 600 cycle PE) to facilitate genome assembly. In brief, gDNA was extracted
239 using a Quick-DNA Microprep Kit (Zymo, cat# D4074) from 10 pooled females for each species
240 and quantified on a Qubit 2.0 (Invitrogen). These samples were sent to the University of
241 Michigan DNA Sequencing Core to prepare 300 bp paired-end libraries, which were quantified
242 by qPCR and sequenced in a single lane of Illumina MiSeq.
243
244 *Genome assembly*
245
246 In brief, Illumina reads from all 965 backcross recombinants were used to perform MSG on the
247 Baylor College of Medicine *D. elegans* genome assembly (accession number:
248 GCA_000224195.2). Using custom scripts in R and Python
249 (https://github.com/masseyj/elegans), the recombination fraction between the Baylor and MSG

contigs was calculated and plotted to manually tabulate joins and splits between newly assembled contigs. These new contigs were then used to assemble approximately chromosome length scaffolds in *D. elegans* (accession number: PRJNA590036) and partially assembled chromosomes in *D. gunungcola* (accession number: PRJNA590037).

Marker generation with Multiplexed Shotgun Genotyping

Following methods described previously (Andolfatto *et al*., 2011; Cande *et al*., 2012), we used the MSG software pipeline (https://github.com/JaneliaSciComp/msg/tree/master/instructions) to perform data parsing and chromosome ancestry estimation to generate markers for quantitative trait locus (QTL) analysis. In brief, using data from the Illumina backcross sequencing library (see Supplementary File S2 for the number of reads per individual), we mapped reads to the assembled *D. elegans* and *D. gunungcola* parental genomes to estimate chromosome ancestry for each backcross individual. We generated 3,425 and 3,121 markers for the *D. elegans* and *D. gunungcola* backcrosses, respectively (Supplementary Files S3, S4), for QTL analysis. PDFs of chromosomal breakpoints for each recombinant are available here: https://deepblue.lib.umich.edu/data/concern/data_sets/j098zb17n?locale=en.

QTL analysis

QTL analysis was performed using R/qtl (Broman *et al*., 2003) in R for Mac version 3.3.3 (R Core Team 2018) in a MacOS environment. Ancestry data for both backcross directions were

imported into R/qtl using a custom script (https://github.com/dstern/read_cross_msg), which directly imports the conditional probability estimates produced by the Hidden Markov Model (HMM) of MSG (Andolfatto *et al*., 2011). We performed genome scans with a single QTL model using the "scanone" function of R/qtl and Haley-Knott regression (Haley and Knott, 1992) for "Wing spot size" and "Maximum wing display angle". Note, for "Wing spot size", 68 and 42 recombinants from the *D. elegans* and *D. gunungcola* backcross populations, respectively, were excluded from the QTL mapping because their wings were too damaged to quantify spot variation. Similarly, for "Maximum wing display angle", 314 and 94 recombinants were excluded from the QTL mapping because these males did not perform any courtship behavior during the assay. Significance of QTL peaks at $\alpha = 0.01$ was determined by performing 1000 permutations of the data. Effect sizes for each QTL peak were individually estimated by comparing the mean "Wing spot size" or "Maximum wing display angle" between individuals that inherited either *D. elegans* or *D. gunungcola* alleles at each QTL peak position.

Since we detected multiple QTL peaks on separate chromosomes for "Maximum wing display angle", we tested for the presence of epistatic interactions using two methods: First, we performed two- and three-way ANOVAs comparing the effect of each QTL peak in multiple QTL peak genetic backgrounds and found no evidence of an interaction. For two-way ANOVAs, we tested for any statistically significant interactions for max wing display angles between two different QTL peaks in the *D. elegans* backcross. For three-way ANOVAs, we tested for any statistically significant interactions for max wing display angles between three different QTL peaks in the *D. gunungcola* backcross. Second, we performed genome-wide pairwise tests using the "scantwo" function of R/qtl and Haley-Knott regression to test for non-additive interactions

296 across all markers; LOD significance thresholds at α = 0.05, 0.01, and 0.001 were determined by
297 performing 1000 permutations of the data for each model (Supplementary Figure S2,
298 Supplementary Tables S1,S2).
299
300 *Annotating the wing spot QTL interval*
301
302 To annotate genes within the ~440 Kbp fine-mapped wing spot locus, we performed nucleotide
303 BLAST (BLASTn) (Johnson *et al*., 2008) searches against the *D. melanogaster* genome (taxid:
304 7227) using ~10 Kbp windows of assembled *D. elegans* chromosomal regions spanning the wing
305 spot QTL interval. Using the "GBrowse" tool on Flybase (Thurmond *et al*., 2018), we mapped
306 regions of microsynteny to identify the orientation of each gene and exported the respective *D.*
307 *melanogaster* coding region (CDS) FASTA sequences to align with the *D. elegans* X
308 chromosome.
309
310 *In situ hybridization*
311
312 Fly genomic DNA (gDNA) was extracted from ten homogenized *D. elegans* and *D. gunungcola*
313 females using a Quick-DNA Microprep Kit (Zymo, cat# D3021). The following forward and
314 reverse primers were designed and synthesized by Integrated DNA Technologies (IDT) to PCR
315 amplify 321 bp DNA templates targeting exon 5 of the *omb* locus in *D. elegans*: 5'-
316 GCTGAGGATCCATTCGCTAGATTTG-3' and 5'-GTTGTTGGAACTAGAGTTGTTGGTG-
317 3', and *D. gunungcola*: 5'- GCTGAGGATCCATTCGCTAGATTTG-3' and 5'-
318 GTTGTTGGAACTGGAGTTGTTGGTG-3'. Reverse primers were designed beginning with a

T7 RNA polymerase binding sequence (TAATACGACTCACTATAG) to facilitate *in vitro* transcription. Raw PCR products were then used to generate digoxigenin-labeled RNA probes using a T7 RNA *in vitro* transcription kit (Promega / Life Technologies). RNA was ethanol precipitated and resuspended in water to analyze on a Nanodrop. Each probe was stored at -20ºC in 50% formamide before *in situ* hybridization.

All tissues underwent primary dissection in PBS, fixed for 30 mins in 4% PFA, washed 3X in PBT and underwent secondary dissection in PBT, were then washed 2X in MeOH, and 2X in EtOH before being stored at -20C. Male *D. elegans* and *D. gunungcola* L3 wing discs were dissected first to validate that our *omb* probes detected an mRNA expression pattern similar to *D. melanogaster* (Grimm and Pflugfelder, 1996; Supplementary Figure S3). Next, pupal wings were dissected at 30 and 48 h after pupal formation (APF) to probe for *omb* mRNA. To prepare pupal wings, appropriately staged pupae underwent a primary dissection: were cut in half along the anterior-posterior axis using Astra Platinum Double Edge Razor Blades, and fat body was washed out of the pupal casing using a pipette and PBS prior to fixation. After fixation, pupal wings underwent a secondary dissection to pull off the cuticle surrounding each wing and then washed using the procedure described above. Finally, *in situ* hybridization was carried out as previously described (Vincent *et al*., 2019). Briefly, we used an InsituPro VSi robot to rehydrate in PBT, fix in PBT with 4% PFA, and prehybridize in hybridization buffer for 1 hr at 65˚C. Samples were then incubated with probe for 16 h at 65˚C before washing with hybridization buffer and PBT. Samples were blocked in PBT with 1% bovine serum albumin (PBT+BSA) for 2 hours. Samples were then incubated with anti-digoxigenin Fab fragments conjugated to alkaline phosphatase (Roche) diluted 1:6000 in PBT+BSA. After additional washes, color

342 reactions were performed by incubating samples with NBT and BCIP (Promega) until purple
343 stain could be detected under a dissecting microscope. Samples were mounted in glycerol on
344 microscope slides coated with poly-L-lysine and imaged at 10X magnification on a Leica
345 DFC450C camera.
346
347 *Generating advanced recombinant introgressions on the X chromosome*
348
349 To try to isolate the QTL effects for "Wing spot size" and "Maximum wing display angle"
350 localized to the X chromosome according to the *D. elegans* backcross experiment, F_1 hybrid
351 females were generated using the procedures described above. F_1 hybrid females were then
352 backcrossed to *D. elegans* males, and backcross males lacking wing spots were isolated to
353 measure "Maximum wing display angles" during courtship as described above. This procedure
354 was repeated for seven generations to generate BC3-BC9 backcross individuals: backcross
355 females were backcrossed en masse to *D. elegans* males, and BC3 backcross males lacking wing
356 spots were isolated to measure "Maximum wing display angles" during courtship with *D.*
357 *elegans* virgins (and so on to BC9). At each generation, an attempt was made to create stable
358 introgression lines of advanced recombinant males lacking wing spots, but all failed to produce
359 offspring, suggesting that *D. gunungcola* X-linked loci might also contain hybrid sterility factors.
360 After seven generations of backcrossing, gDNA from all backcross males lacking wing spots was
361 extracted and sequenced for MSG as described above. Backcross males lacking wing spots from
362 BC4-BC9 were homozygous for *D. elegans* genomic regions across all autosomes but varied for
363 the amount of *D. gunungcola* genome regions on the X chromosome.
364

365 *Introgression of black body color alleles from* D. gunungcola *into* D. elegans

366

367 In the *D. gunungcola* backcross, QTL mapping for wing spot size revealed QTL peaks linked to
368 Muller Element C and E when spotless recombinants were excluded from the analysis
369 (Supplementary Figure S4; Supplementary Table S3). The Muller Element E QTL peak is
370 located near the *ebony* gene, which appears to contribute to variation in body color between *D.*
371 *elegans* and *D. gunungcola* (unpublished data). We therefore reasoned that introgressing dark
372 body color from *D. gunungcola* into *D. elegans* would introgress the Muller Element E QTL
373 peak underlying wing spot size differences. After six generations of backcrossing dark brown
374 female recombinants with *D. elegans* males, we crossed dark brown male and female
375 recombinants together to create black offspring homozygous for the introgressed region. We then
376 performed MSG on a single, dark black introgression line and found that it was homozygous for
377 ~1.5 Mb of *D. gunungcola* alleles linked near the Muller Element E QTL peak (Supplementary
378 Figure S4A,B).

379

380 Observing and collecting wild *D. gunungcola* in Indonesia

381

382 Throughout early July 2018, *D. elegans* and *D. gunungcola* were recorded performing courtship
383 in East Java, Indonesia on *Brugmansia sp.* flowers using Canon VIXIA HF R500 camcorders
384 mounted to Manfrotto (MKCOMPACTACN-BK) aluminum tripods. Both species were observed
385 in sympatry on flowers near Coban Rondo Waterfall in Batu, Batu City, East Java, Indonesia (-
386 7.884985, 112.477311). After observing courtship, males and females were captured using a
387 mouth pipette and gently aspirated into glass vials containing standard fly media (glucose, corn

meal, yeast extract, and agar). Isofemale lines of *D. gunungcola* from Bumiaji District (Batu City, East Java Province, Indonesia) were established in the laboratory on standard fly media at 24°C temperature.

Statistics

Statistical tests were performed in R for Mac version 3.3.3 (R Core Team 2018) using Student's t-test (two-tailed) to test for statistically significant effects of pairwise comparisons of continuous data with normally distributed error terms. For tests comparing more than two groups, ANOVAs were performed with *post hoc* Tukey HSD for pairwise comparisons adjusted for multiple comparisons. See "QTL analysis" methods for statistical tests used during QTL mapping.

Results and Discussion

X-linked sequence divergence contributed to wing spot and wing display divergence

D. elegans males perform elaborate wing display dances (Video 1) in front of females during courtship, displaying the presence of darkly pigmented wing spots (Figure 1B), whereas its sibling species, *D. gunungcola*, lacks wing spots (Yeh *et al.*, 2006; Prud'homme *et al*., 2006) and wing displays (Figure 1B; Video 2). Despite these differences in sexual traits, *D. elegans* and *D. gunungcola* can mate and form viable F_1 hybrids in the lab (Yeh *et al*., 2006; Yeh and True, 2014). Sequence divergence on the X chromosome has previously been implicated in the divergence of wing spots and wing display behavior (Yeh *et al*., 2006; Yeh and True, 2014). To

confirm this effect of the X-chromosome, we quantified variation in wing spot size and wing display behavior in F_1 hybrid males from reciprocal crosses between *D. elegans* and *D. gungungcola*. These F_1 hybrids inherited their X chromosome from either *D. elegans* or *D. gunungcola* (whichever species was their mother) and autosomes from both species. Consistent with prior work, F_1 hybrid males inheriting the X chromosome from *D. elegans* mothers (F_1E) possessed wing spots, whereas F_1 hybrid males inheriting the X chromosome from *D. gunungcola* mothers (F_1G) did not (Figure 1C,D). These wing spots of F_1E males were smaller, however, than the wing spots seen in *D. elegans* (Figure 1D, test, $P = 0.02$). Differences in wing display behavior were also apparent between F_1E (Video 3) and F_1G hybrids (Video 4), which is also consistent with prior work (Yeh *et al*., 2006; Yeh and True, 2014). More specifically, we found that although both F_1 hybrids performed wing displays during courtship, F_1E hybrids tended to open their wings more widely than F_1G hybrids during display performance (Figure 1C). We quantified variation in this wing display trait between F_1 hybrids by measuring the maximum bilateral wing display angles (Figure 1C) during courtship (see Methods). We found that F_1E hybrids performed wing displays comparable to *D. elegans* males (Figure 1E, post-hoc Tukey HSD, $P = 0.6$), whereas F_1G males showed, on average, lower display angles (Figure 1E, post-hoc Tukey HSD, $P = 7.1 \times 10^{-5}$). Together these data confirm that divergence of one or more loci on the X chromosome contribute to divergence in wing spot size and wing display behavior between *D. elegans* and *D. gunungcola.*

Evolution of at least three loci contribute to wing spot divergence

To identify the location of X-linked (as well as autosomal) loci contributing to divergence in wing spot size, we quantified wing spot size variation in 656 recombinant males produced by backcrossing F_1 hybrid females to *D. elegans* males and 199 recombinant males produced by backcrossing F_1 hybrid females to *D. gunungcola* males. These backcross males showed a range of wing spot sizes (Figure 2A). Using Multiplexed Shotgun Genotyping (MSG) (Andolfatto *et al*., 2011), we inferred the allele most likely inherited from the F_1 mother (*D. elegans* or *D. gunungcola*) for each genomic position in each recombinant. We then performed quantitative trait locus (QTL) mapping for wing spot size and identified a single, highly significant QTL peak on the X chromosome (Figure 2B and Table 1). In both backcross directions, variation linked to this wing spot QTL peak explained almost all of the difference in wing spot size between *D. elegans* and *D. gunungcola* (Figure 2C). Repeating the QTL mapping after excluding recombinant individuals lacking wing spots, however, allowed us to identify additional QTLs of smaller effect on Muller Elements C (chromosome 2R in *D. melanogaster*) and E (chromosome 3R in *D. melanogaster*) in the *D. gunungcola* (but not *D. elegans*) backcross population (Supplementary Figure S4A; Supplementary Table S3). Observing these QTL only in the *D. gunungcola* backcross populations suggests that they are caused by recessive *D. gunungcola* alleles, which are never homozygous in the *D. elegans* backcross population. Introgressing the QTL region on Muller Element E from *D. gunungcola* into *D. elegans* through 5 generations of backcrossing (Supplementary Figure S4C) reduced the size of wing spots (Supplementary Figure S4D, E). This region includes the *ebony* gene, which has previously been shown to be able to inhibit the development of dark pigments in *D. melanogaster* (Wittkopp *et al.*, 2002b). Crossing this introgression line to *D. elegans* masked most of the reduction in spot size (Supplementary Figure 4D, E), consistent with the *D. gunungcola* QTL allele being recessive to the *D. elegans*

456 allele. Taken together, these data indicate that the majority of wing spot divergence between *D.*
457 *elegans* and *D. gunungcola* maps to a single, large-effect QTL on the X chromosome, but that
458 wing spot size is also influenced by loci on Muller Elements C and E.
459
460 *A 440 kb locus behaves like a genetic switch for wing spots*
461
462 To further refine the X-linked QTL, we more closely examined the genotypes and phenotypes of
463 recombinants with inferred crossover positions immediately flanking the wing spot QTL peak
464 (Figure 2D, Supplementary Figure S5). Doing so allowed us to identify a ~440 kb region
465 containing a QTL that acts like a genetic switch controlling the presence or absence of the wing
466 spot (Figure 2D, Supplementary Figure S5). This region includes 15 genes (Figure 2E) and
467 notably excludes the X-linked pigmentation gene, *yellow*, which has previously been suggested
468 to contribute to wing spot development and evolution (Wittkopp *et al*., 2002a; Gompel *et al*.,
469 2005; Prud'homme *et al*., 2006; Yeh *et al*., 2006; Arnoult *et al*., 2013; Yeh and True, 2014;
470 Supplementary Figure 6). One of these 15 genes is *optomotor-blind* (*omb*) (Figure 2E), which
471 encodes a T-box-containing transcription factor (Pflugfelder *et al*., 1992a; Pflugfelder *et al*.,
472 1992b) that has previously been implicated in pigmentation patterning (Thompson, 1959; Kopp
473 and Duncan, 1997), pigmentation evolution (Brisson *et al*., 2004), and distal wing patterning
474 (Grim and Pflugfelder, 1996). In *D. melanogaster*, gain- and loss-of-function *omb* alleles cause
475 expansion and contraction of abdominal pigmentation bands, respectively (Kopp and Duncan,
476 1997), and variation in abdominal pigmentation in *D. polymorpha* is strongly associated with
477 polymorphisms at the *omb* locus (Brisson *et al*., 2004).
478

Although we identified two nonsynonymous protein coding changes between *D. elegans* and *D. gunungcola* (Supplementary File S5), *omb* is required for the development of many structures throughout the body (Pflugfelder, 2009); we, therefore, reasoned that genetic divergence in *omb* would be more likely to affect its expression than its protein function (Stern and Orgogozo, 2008). To look for differences in *omb* expression between *D. elegans* and *D. gunungcola* that might affect wing spot development, we used *in situ* hybridization to detect *omb* mRNA in the developing wing of both species (Figure 2F). In *D. melanogaster*, *omb* is expressed in a broad stripe that overlaps the wing pouch region in larval L3 wing discs (Grimm and Pflugfelder, 1996). *omb* expression in the wing pouch is required for distal wing development, as demonstrated by *D. melanogaster omb* hypomorphs that show disrupted distal wing tip development in adults (Grimm and Pflugfelder, 1996). We hypothesized, therefore, that differences in *D. elegans* and *D. gunungcola omb* expression patterning during pupal wing development might prefigure changes in wing spot pigmentation observed in adult males, similar to the changes in *wingless* expression shown to prefigure wing spots in *D. guttifera* (Werner *et al.*, 2010). Consistent with the expression of *omb-lacZ* in pupal wings of *D. melanogaster* (Álamo Rodríguez *et al*., 2004), we detected *omb* mRNA in the wing hinge and distal wing tip 30 h after puparium formation (APF) in *D. elegans* and *D. gunungcola* (Figure 2F). We were unable to identify any consistent differences in the *omb* expression patterns between *D. elegans* and *D. gunungcola* although it is possible that w e may not have detected subtle differences in expression patterns. In addition, it is possible that the changes in *omb* protein sequence contribute to differences in wing spot patterning, or that other genes in the minimal mapped interval are the true cause of the difference in wing spot patterning.

Evolution at multiple loci contributed to wing display divergence

To identify loci contributing to divergence in wing display behavior, we quantified variation in maximum wing display angles (see Methods) in 410 *D. elegans* and 147 *D. gunungcola* backcross recombinant males, again observing a range of phenotypes (Figure 3A). We identified multiple significant QTL contributing to variation in wing display (Figure 3B; Table 1). In the *D. elegans* backcross, we mapped a QTL on the X chromosome that co-localized with the wing spot QTL (Figure 3B,E; Table 1). We also mapped a QTL on Muller Element B (chromosome 2L in *D. melanogaster*) (Figure 3B; Table 1). In the *D. gunungcola* backcross, we mapped QTLs on the X chromosome as well as Muller Elements B and E (Figure 2E; Table 1). These differences in QTL peaks mapped using backcrosses to *D. elegans* and *D. gunungcola* suggest that *D. elegans* and *D. gunungcola* alleles affecting wing display behavior are recessive and/or interact epistatically with divergent sites elsewhere in the genome.

To test for epistatic interactions contributing to wing display divergence, we performed a two-dimensional genome scan to search for non-additive interactions across all markers in both backcross directions and found no significant interactions (Supplementary Figure S2; Supplementary Tables S1,S2). We also tested for evidence of non-additive interactions among the wing display QTL peaks themselves by performing two- and three-way ANOVAs in the *D. elegans* and *D. gunungcola* backcrosses, respectively, and found no evidence of significant interactions between loci (Figure 3C). Instead, each wing display QTL peak appears to behave approximately additively, with *D. gunungcola* alleles contributing to lower maximum wing display angles (Figure 3C). Surprisingly, the effect of the X-linked QTL on wing display angle in

the *D. gunungcola* backcross in multiple genetic backgrounds was similar to the estimated effect size of the X-linked QTL in the *D. elegans* backcross (compare panels in Figure 3C) despite the much lower LOD score of the X-linked QTL in the *D. gunungcola* backcross population (Figure 3B; Table 1). We suggest that while the detected QTL in the *D. gunungcola* backcross appear to interact additively with each other, undetected QTL elsewhere in the genome are likely masking the X-effect in the *D. gunungcola* backcross map. While the purpose of the two-dimensional genome scan (Supplementary Figure S2; Supplementary Tables S1,S2) was to detect these effects, our sample size is likely too small to identify small-effect epistatic interactions.

Males lacking wing spots perform normal wing displays

While it remains unclear which gene evolved to cause the majority of wing spot divergence, fine-mapping the locus controlling the presence or absence of the wing spot allowed us to test whether the locus that turns off wing spots in *D. gunungcola* also affects wing display behavior. To perform this test, we introgressed *D. gunungcola* alleles causing a loss of the wing spot into *D. elegans* by repeated backcrossing (see Methods). We recovered three introgression lines lacking wing spots and found that all three lines had inherited the ~440 kb region observed in mapping experiments to act like a genetic switch controlling wing spot development (Figure 4A,B), independently confirming the causal role of the switch region in wing spot divergence. We noticed, however, that several advanced recombinants developed a wing spot "shadow" (Figure 4B), possibly due to the effects of other *D. elegans* alleles affecting wing spot development. We next asked whether the spotless advanced recombinants performed wing displays with lower wing display angles than *D. elegans* males. Surprisingly, we found that all

548 advanced recombinants inheriting the *D. gunungcola* allele eliminating the wing spot performed
549 wing displays indistinguishable from *D. elegans* males during courtship (Figure 4B,C; Videos 5-
550 7). Thus, the loci controlling the wing spot and courtship behavior are genetically separable.
551
552 The repeated co-evolution of male-specific wing spots and wing display behavior in multiple
553 species (Kopp and True, 2002) combined with the presence of overlapping QTL for these traits
554 on the X chromosome (Yeh *et al*., 2006; Yeh and True, 2014; and this study) suggested that a
555 single pleiotropic gene might be contributing to the evolution of both traits. The finding that *D.*
556 *elegans* introgression lines lacking a wing spot performed a normal wing display argues against
557 this hypothesis and indicates instead that these two traits arose independently between this
558 species pair. To further investigate how these divergent traits might have evolved, we observed
559 courtship behavior in a wild population of *D. gunungcola* in Indonesia; to the best of our
560 knowledge, all prior studies of *D. gunungcola* pigmentation and courtship used the one
561 previously available lab strain (Sultana *et al*., 1999). Surprisingly, we found that all *D.*
562 *gunungcola* males observed in the wild population sampled lacked wing spots (Supplementary
563 Figure 7) but performed wing displays (Videos 8,9), confirming that these are genetically distinct
564 traits. The wing displays performed by these flies appeared to show a lower maximum wing
565 extension angle than *D. elegans* (Videos 1,10), similar to the wing display behavior seen in F1
566 hybrids between *D. elegans* and *D. gunungcola* with *D. gunungcola* mothers (Video 4). Analysis
567 of new lab strains founded by flies captured from this *D. gunungcola* population showed similar
568 male courtship behavior in the lab as observed on flowers (Video 11). We therefore conclude
569 that although the absence of wing spots appears fixed in *D. gunungcola*, the absence of wing
570 display behavior does not. It remains to be seen whether the lack of wing display in the strain

571 collected in 1999 resulted from polymorphic alleles segregating within *D. gunungcola* or a
572 change that occurred since this strain was brought into the laboratory. Assuming that the loss of
573 the wing spot and wing display behavior are derived traits in *D. gunungcola* (Prud'homme *et al.*,
574 2006), these observations suggest that the loss of male-specific wing spots predates the loss of
575 male wing display behavior in this species.
576
577 **Conclusions**
578
579 Male-specific wing spots and wing display behavior have co-evolved in *Drosophila* multiple
580 times (Kopp and True, 2002). By studying the genetic basis of these divergent traits between *D.*
581 *elegans* and *D. gunungcola*, we showed that the changes in wing spot and wing display were not
582 caused by changes in a single, pleiotropic gene despite overlapping QTL (Yeh *et al*., 2006; Yeh
583 and True, 2014). Rather, we found that distinct loci contribute to divergence in each of these
584 traits, with the genetic architecture of divergent wing behavior being more complex than that of
585 the divergent wing spot pigmentation. Both traits were affected by divergent gene(s) located on
586 the X chromosome that are in physical linkage, however, causing alleles of these distinct loci to
587 be co-inherited. This linkage might have facilitated the coordinated evolution of these traits.
588
589 The specific genes contributing to divergence in wing spot and wing display remain unknown,
590 but *optomotor-blind* is a strong candidate for the X-linked gene contributing to the loss of the
591 wing spot. Introgression lines and additional sampling of *D. gunungcola* from a wild population
592 also showed that the loss of wing spots and wing display are not inexorably linked: in both cases,
593 males lacking wing spots still performed a wing display behavior. Coordinated evolution of

morphological and behavioral traits such as these is often observed in animal species, but it is often unclear which change evolved first. In this case at least, it seems that the divergence of morphology preceded the divergence of behavior.

Acknowledgements

We thank members of the Wittkopp, Stern, and Rebeiz labs for helpful discussions. For fly strains, we thank John True (Stony Brook University). For guidance throughout the *in situ* hybridization work, we thank Mark Rebeiz (University of Pittsburgh). For arranging the Material Transfer Agreement for *D. gunungcola* and *D. elegans*, we thank Nia Kurniawan (University of Brawijaya, Indonesia); for hosting us in Indonesia, we thank Karuniawan Wicaksono (University of Brawijaya, Indonesia); for assistance with field collections, we thank Hagus Tarno (University of Brawijaya, Indonesia). Funding: University of Michigan, Department of Ecology and Evolutionary Biology, Peter Olaus Okkelberg Research Award, National Institutes of Health (NIH) training grant T32GM007544, and Howard Hughes Medical Institute Janelia Graduate Research Fellowship to J.H.M.; NIH R01 GM089736 and 1R35GM118073 to PJW.

Author Contributions

Jonathan H. Massey, Conceptualization, Data curation, Formal analysis, Funding acquisition, Validation, Investigation, Visualization, Methodology, Writing—original draft, Writing—review and editing; Gavin R. Rice, Formal analysis, Validation, Investigation, Methodology, Writing—review and editing; Anggun Firdaus, Investigation, Methodology, Writing—review and editing; Chi-Yang Chen, Investigation, Methodology; Shu-Dan Yeh, Funding acquisition, Investigation,

Methodology; David L. Stern, Supervision, Funding acquisition, Conceptualization, Data curation, Formal analysis, Investigation, Visualization, Writing—original draft, Project administration, Writing—review and editing; Patricia J. Wittkopp, Supervision, Funding acquisition, Conceptualization, Data curation, Formal analysis, Investigation, Visualization, Writing—original draft, Project administration, Writing—review and editing.

References

Andolfatto, P., Davison, D., Erezyilmaz, D., Hu, T. T., Mast, J., Sunayama-Morita, T., & Stern, D. L. (2011). Multiplexed shotgun genotyping for rapid and efficient genetic mapping. *Genome Research*, *21*(4), 610-617.

Álamo Rodríguez, D., Felix, J. T., & Díaz-Benjumea, F. J. (2004). The role of the T-box gene optomotor-blind in patterning the Drosophila wing. *Developmental Biology*, *268*(2), 481-492.

Arnoult, L., Su, K. F., Manoel, D., Minervino, C., Magriña, J., Gompel, N., & Prud'homme, B. (2013). Emergence and diversification of fly pigmentation through evolution of a gene regulatory module. *Science*, *339*(6126), 1423-1426.

640 Bock, I. R., and Wheeler, M. R. (1972) The *Drosophila melanogaster* species group.
641 University of Texas Publication 7213, 1–102.
642
643 Brisson, J. A., Templeton, A. R., & Duncan, I. (2004). Population genetics of the
644 developmental gene *optomotor-blind* (*omb*) in *Drosophila polymorpha*: evidence
645 for a role in abdominal pigmentation variation. *Genetics*, *168*(4), 1999-2010.
646
647 Broman KW, Wu H, Sen S, Churchill GA (2003) R/qtl: QTL mapping in experimental
648 crosses. *Bioinformatics*, *19*: 889–890.
649
650 Broman, K. W., & Sen, S. (2009). A Guide to QTL Mapping with R/qtl (Vol. 46). New
651 York: Springer.
652
653 Cande, J., Andolfatto, P., Prud'homme, B., Stern, D. L., & Gompel, N. (2012). Evolution
654 of multiple additive loci caused divergence between *Drosophila yakuba* and *D.*
655 *santomea* in wing rowing during male courtship. *PLoS One*, *7*(8), e43888.
656
657 Charlesworth, D., & Charlesworth, B. (1976). Theoretical genetics of Batesian mimicry
658 II. Evolution of supergenes. *Journal of Theoretical Biology*, *55*(2), 305-324.
659
660 Endler, J. A. (1991). Variation in the appearance of guppy color patterns to guppies and
661 their predators under different visual conditions. *Vision Research*, *31*(3), 587-608.
662

663 Gompel, N., Prud'homme, B., Wittkopp, P. J., Kassner, V. A., & Carroll, S. B. (2005).
664 Chance caught on the wing: cis-regulatory evolution and the origin of pigment
665 patterns in *Drosophila*. *Nature*, *433*(7025), 481.
666
667 Gray, S. M., & McKinnon, J. S. (2007). Linking color polymorphism maintenance and
668 speciation. *Trends in Ecology & Evolution*, *22*(2), 71-79.
669
670 Grimm, S. and Pflugfelder, G. O. (1996). Control of the gene *optomotor-blind* in
671 *Drosophila* wing development by *decapentaplegic* and *wingless*. *Science*, *271*,
672 1601-04.
673
674 Haley CS, Knott SA (1992). A simple regression method for mapping quantitative trait
675 loci in line crosses using flanking markers. *Heredity*, *69*: 315–324.
676
677 Johnson, M., Zaretskaya, I., Raytselis, Y., Merezhuk, Y., McGinnis, S., & Madden, T. L.
678 (2008). NCBI BLAST: a better web interface. Nucleic Acids Research,
679 36(suppl_2), W5-W9.
680
681 Kirkpatrick, M., & Barton, N. (2006). Chromosome inversions, local adaptation and
682 speciation. *Genetics*, *173*(1), 419-434.
683
684 Kopp, A., & Duncan, I. (1997). Control of cell fate and polarity in the adult abdominal
685 segments of *Drosophila* by *optomotor-blind*. *Development*, *124*(19), 3715-3726.

Kopp, A., & True, J. R. (2002). Evolution of male sexual characters in the oriental *Drosophila melanogaster* species group. *Evolution & Development*, *4*(4), 278-291.

Kronforst, M. R., Young, L. G., Kapan, D. D., McNeely, C., O'Neill, R. J., & Gilbert, L. E. (2006). Linkage of butterfly mate preference and wing color preference cue at the genomic location of wingless. *Proceedings of the National Academy of Sciences*, *103*(17), 6575-6580.

Küpper, C., Stocks, M., Risse, J. E., dos Remedios, N., Farrell, L. L., McRae, S. B., ... & Kitaysky, A. S. (2016). A supergene determines highly divergent male reproductive morphs in the ruff. *Nature Genetics*, *48*(1), 79.

Lamichhaney, S., Fan, G., Widemo, F., Gunnarsson, U., Thalmann, D. S., Hoeppner, M. P., ... & Chen, W. (2016). Structural genomic changes underlie alternative reproductive strategies in the ruff (Philomachus pugnax). *Nature Genetics*, *48*(1), 84.

Lindholm, A., & Breden, F. (2002). Sex chromosomes and sexual selection in poeciliid fishes. *The American Naturalist*, *160*(S6), S214-S224.

Loxton, R. G. (1979). On display behaviour and courtship in the praying mantis

Ephestiasula amoena (Bolivar). *Zoological Journal of the Linnean Society*, *65*(1), 103-110.

McKinnon, J. S., & Pierotti, M. E. (2010). Colour polymorphism and correlated characters: genetic mechanisms and evolution. *Molecular Ecology*, *19*(23), 5101-5125.

Merrill, R. M., Rastas, P., Martin, S. H., Melo, M. C., Barker, S., Davey, J., ... & Jiggins, C. D. (2019). Genetic dissection of assortative mating behavior. *PLoS Biology*, 17(2), e2005902.

Pflugfelder, G. O., Roth, H. and Poeck, B. (1992a). A homology domain shared between *Drosophila optomotor-blind* and mouse Brachyury is involved in DNA binding. *Biochem. Biophys. Res. Comm*., *186*, 918-25.

Pflugfelder, G. O., Roth, H., Poeck, B., Kersher, S., Schwarz, H., Jonschker, B. and Heisenberg, M. (1992b). The lethal (1) *optomotor-blind* gene of *Drosophila melanogaster* is a major organizer of optic lobe development: Isolation and characterization of the gene. *Proc. Nat. Acad. Sci*., *89*, 1199-1203.

Pflugfelder, G. O. (2009). omb and circumstance. *Journal of neurogenetics*, *23*(1-2), 15-33.

Picelli, S., Björklund, Å. K., Reinius, B., Sagasser, S., Winberg, G., & Sandberg, R. (2014). Tn5 transposase and tagmentation procedures for massively scaled

732 sequencing projects. *Genome Research*, *24*(12), 2033-2040.

733

734 Prud'Homme, B., Gompel, N., Rokas, A., Kassner, V. A., Williams, T. M., Yeh, S. D., ...

735 & Carroll, S. B. (2006). Repeated morphological evolution through cis-regulatory

736 changes in a pleiotropic gene. *Nature*, *440*(7087), 1050-1053.

737

738 R Core Team. 2013. R: A Language and Environment for Statistical Computing. Available from:

739 http://www.r-project.org/.

740

741 Simon, J. C., & Dickinson, M. H. (2010). A new chamber for studying the behavior of

742 *Drosophila*. *Plos One*, 5(1), e8793.

743

744 Sinervo, B., Miles, D. B., Frankino, W. A., Klukowski, M., & DeNardo, D. F. (2000).

745 Testosterone, endurance, and Darwinian fitness: natural and sexual selection on

746 the physiological bases of alternative male behaviors in side-blotched

747 lizards. *Hormones and Behavior*, *38*(4), 222-233.

748

749 Stern, D. L., & Orgogozo, V. (2008). The loci of evolution: how predictable is genetic

750 evolution?. *Evolution*, *62*(9), 2155-2177.

751

752 Sultana, F., Kimura, M. T., & Toda, M. J. (1999). Anthophilic *Drosophila* of the *elegans*

753 species-subgroup from Indonesia, with description of a new species (Diptera:

754 Drosophilidae). *Entomological Science*, *2*, 121-126.

Thomas, J. W., Cáceres, M., Lowman, J. J., Morehouse, C. B., Short, M. E., Baldwin, E. L., ... & Martin, C. L. (2008). The chromosomal polymorphism linked to variation in social behavior in the white-throated sparrow (*Zonotrichia albicollis*) is a complex rearrangement and suppressor of recombination. *Genetics*, *179*(3), 1455-1468.

Thompson, P. E. (1959). Drosophila. Info. Service 33, 99

Thurmond, J., Goodman, J. L., Strelets, V. B., Attrill, H., Gramates, L. S., Marygold, S. J., ... & Kaufman, T. C. (2018). FlyBase 2.0: the next generation. *Nucleic Acids Research*, *47*(D1), D759-D765.

Vincent, B. J., Rice, G. R., Wong, G. M., Glassford, W. J., Downs, K. I., Shastay, J. L., ... & Rebeiz, M. (2019). An atlas of transcription factors expressed in male pupal terminalia of *Drosophila melanogaster*. *G3: Genes, Genomes, Genetics*, g3-400788.

Werner, T., Koshikawa, S., Williams, T. M., & Carroll, S. B. (2010). Generation of a novel wing colour pattern by the Wingless morphogen. *Nature*, *464*(7292), 1143.

Wirtz, R. A. and Semey, H. G. (1982). The Drosophila kitchen - equipment, media preparation, and supplies. *Drosophila Information Service*. *58*, 176-180.

White, T. E., Zeil, J., & Kemp, D. J. (2015). Signal design and courtship presentation coincide for highly biased delivery of an iridescent butterfly mating signal. *Evolution*, *69*(1), 14-25.

Wittkopp, P. J., Vaccaro, K., & Carroll, S. B. (2002a). Evolution of *yellow* gene regulation and pigmentation in *Drosophila*. *Current Biology*, *12*(18), 1547-1556.

Wittkopp, P. J., True, J. R., & Carroll, S. B. (2002b). Reciprocal functions of the Drosophila *yellow* and *ebony* proteins in the development and evolution of pigment patterns. *Development*, *129*(8), 1849-1858.

Yeh, S. D., Liou, S. R., & True, J. R. (2006). Genetics of divergence in male wing pigmentation and courtship behavior between Drosophila elegans and D. gunungcola. Heredity, 96(5), 383.

Yeh, S. D., & True, J. R. (2014). The genetic architecture of coordinately evolving male wing pigmentation and courtship behavior in Drosophila elegans and Drosophila gunungcola. G3: Genes, Genomes, Genetics, 4(11), 2079-2093.

Figure Legends

Figure 1 Wing pigmentation and wing display behavior in *D. elegans*, *D. gunguncola*, and F_1 hybrids

(A) Phylogeny of the "Oriental" *Drosophila melanogaster* species group adapted from Kopp and True (2002) and Prud'homme *et al*. (2006). Plus (+) signs indicate species possess wing spots and/or wing displays, and minus (-) signs indicates wing spots and/or wing displays are absent. (B) Males in *D. elegans* (left) possess wing spots and perform bilateral wing display behaviors in front of females during courtship (Video 1). Wing spots and wing displays are absent in *D. gunungcola* males (right) (Video 2). (C) F_1 hybrid males inheriting their X chromosome from *D. elegans* mothers (F_1E, left) possess wing spots and perform wing display behavior like *D. elegans* (Video 3). F_1 hybrid males inheriting their X chromosome from *D. gunungcola* mothers (F_1G, right) are spotless and perform wing displays with low bilateral wing angles (Video 4). (D) Quantification of wing spot size (see Methods) in male *D. elegans* and F_1E. Wing spots are larger in *D. elegans* than F_1E (Student's t-test; t = -2.8057; df = 11.43; P = 0.017; two-tailed). (E) Quantification of maximum bilateral wing display angles during courtship (see Methods) in male *D. elegans* and F_1 hybrids. F_1G hybrids showed lower maximum wing display angles than *D. elegans* and F_1E hybrids (One-way ANOVA: $F_{2,71} = 20.92$; $P < 7.18 \times 10^{-8}$; post-hoc Tukey HSD was significant between *D. elegans* and F_1G: $P < 2.0 \times 10^{-7}$ and between F_1E and F_1G: $P < 7.1 \times 10^{-5}$). Gray triangles represent individual replicates.

Figure 2 QTL analysis, effect plots, and *in situ* hybridization for wing pigmentation divergence

(A) Wing spots vary in size and shape in *D. elegans* and *D. gunungcola* backcross recombinants. Wing spots were traced (pink) and quantified relative to proxies for total wing area (length x width) using ImageJ software (see Methods). (B) Wing spot QTL map for the *D. elegans* (red) and *D. gunungcola* (blue) backcross. LOD (logarithm of the odds) is indicated on the y-axis. The x-axis represents the physical map of Muller Elements X, B, C, D, E, and F based on the *D. elegans* assembled genome (see Methods). While *D. elegans* and *D. gunungcola* have six separate chromosomes (Yeh *et al*., 2006; Yeh and True, 2014), they are each syntenic with the *D. melanogaster* genome accordingly: X = X, B = 2L, C = 2R, D = 3L, E = 3R, F = 4. Individual SNP markers are indicated with black tick marks along the x-axis. Horizontal red and blue lines mark p = 0.01 for the *D. elegans* and *D. gunungcola* backcross, respectively. (C) Effect plots for the X chromosome QTL peak from the *D. elegans* backcross (left) and *D. gunungcola* backcross (right). (D) *D. elegans* and *D. gunungcola* backcross recombinants containing X chromosome breakpoints immediately flanking the wing spot QTL peak were aligned to compare the effects of each on wing pigmentation. Regions in red represent *D. elegans* linked loci, and regions in blue represent *D. gunungcola* linked loci. Recombinants possessing *D. elegans* loci to the left of ~10.32 Mbp are spotless, while recombinants possessing *D. elegans* loci to the right of ~10.74 Mbp possess dark wing spots. (E) Two recombinants define the wing spot locus to a ~440 Kbp region containing 15 candidate genes. *omb* is the strongest wing pigmentation candidate gene given evidence from prior work (see Results and Discussion). (F) *In situ* hybridization of *D. elegans* and *D. gunungcola* pupal wings probed for *omb* mRNA (purple) at 30 h after pupal formation (APF) (see Supplementary Figure S8 for additional replicates). Gray triangles represent individual replicates.

Figure 3 QTL analysis and effect plots for wing display divergence

(A) Maximum wing display angles varied in *D. elegans* and *D. gunungcola* backcross recombinants. Maximum wing display angles were quantified by measuring the angle between each wing tip using ImageJ software (see Methods). (B) Maximum wing display QTL map for the *D. elegans* (red) and *D. gunungcola* (blue) backcross. LOD is indicated on the y-axis. Individual SNP markers are indicated with black tick marks along the x-axis. Horizontal red and blue lines mark P = 0.01 for the *D. elegans* and *D. gunungcola* backcross, respectively. (C) Effect plots for the X chromosome and Muller Element B QTL peaks from the *D. elegans* backcross (left) and for the X, Muller Element B, and E QTL peaks from the *D. gunungcola* backcross (right). No epistatic interactions were detected between QTLs (see Methods) (Two-way ANOVA: $F_{1,402} = 0.146$; P = 0.70 for the *D. elegans* backcross; Three-way ANOVA: $F_{1,137}$ = 0.050 (X:B), 0.034 (X:E), 1.75 (B:E), 0.799 (X:B:E); P = 0.82 (X:B), 0.86 (X:E), 0.19 (B:E), 0.37 (X:B:E) for the *D. gunungcola* backcross). Gray triangles represent individual replicates.

Figure 4 *D. elegans* males possessing the *D. gunungcola* wing spot locus perform normal wing displays

(A) Multiplexed Shotgun Genotyping (MSG) (Andolfatto *et al*., 2011) was used to estimate genome-wide ancestry assignments for three introgression lines generated by repeatedly backcrossing the *D. gunungcola* wing spot QTL region into a *D. elegans* genetic background (see Methods). The posterior probability that a region is homozygous for *D. elegans* (red) or *D. gunungcola* (blue) ancestry is plotted along the y-axis. The dotted line marks the location of the

869 fine-mapped wing spot region (Figure 2D,E; Table 1). (B). None of the introgressions possessed
870 dark wing spots (although a light wing spot "shadow" is visible). (B,C) Every introgression
871 performed max wing display angles indistinguishable from *D. elegans* males (One-way
872 ANOVA: $F_{3,42} = 0.449$; $P = 0.72$). Gray triangles represent individual replicates.
873
874 **Supplementary Figure S1 ImageJ procedure for measuring maximum wing display angles**
875
876 Screenshots of each wing display were captured for every recombinant courtship video. The
877 maximum wing display bout was identified for each fly by quickly comparing screenshots that
878 varied in wing display angles (from wing tip to wing tip) and picking by eye the display with the
879 largest angle. Next, for each fly, the maximum wing display angle was quantified in ImageJ by
880 using 1) Find Edges function, 2) polygon tool to Fit Ellipse around the fly body, 3) Ellipse
881 Macros (Supplementary File S1) to fit the major and minor axes of the ellipse, and 4) draw
882 Angle tool, fitting the angle vertex at the major and minor axes intersection to calculate the wing
883 display angle from wing tip to wing tip.
884
885 **Supplementary Figure S2 LOD scores estimated from a two-dimensional, two QTL scan of**
886 **maximum wing display angles**
887
888 (A) For the *D. elegans* backcross, the Interaction LODi, which estimates the likelihood that the
889 effect of genotypes at one marker depend on genotypes at another, is displayed in the upper left
890 triangle; the Full LODf, which estimates the effect of both additive and non-additive interactions
891 between genotypes (see Supplementary Table S2 for LOD thresholds), is displayed in the lower

892 right triangle (Broman *et al*., 2003). The color scale on the right indicates LOD values for LODi
893 (left) and LODf (right). (B) For the *D. gunungcola* backcross, the Interaction LODi is displayed
894 in the upper left triangle; the Full LODf (see Supplementary Table S3 for LOD thresholds) is
895 displayed in the lower right triangle. The color scale on the right indicates LOD values for LODi
896 (left) and LODf (right).
897
898 **Supplementary Figure S3 *In situ* hybridization of *D. elegans* and *D. gunungcola* L3 wing**
899 **discs**
900
901 Male *D. elegans* (left) and *D. gunungcola* (right) L3 wing discs were dissected and stained with
902 probes targeting *omb* mRNA.
903
904 **Supplementary Figure S4 Effects of Muller Element E on wing spot divergence**
905
906 (A) Wing spot QTL map for *D. elegans* (red) and *D. gunungcola* (blue) backcross recombinants.
907 Note, all recombinant individuals that lacked wing spots were removed from this QTL analysis
908 to identify loci contributing to wing spot size variation independent of wing spot presence or
909 absence. LOD (logarithm of the odds) is indicated on the y-axis. The x-axis represents the
910 physical map of Muller Elements X, B, C, D, E, and F based on the *D. elegans* assembled
911 genome (see Methods). Individual SNP markers are indicated with black tick marks along the x-
912 axis. Horizontal red and blue lines mark P = 0.01 for the *D. elegans* and *D. gunungcola*
913 backcross, respectively. (B) Images illustrating *D. elegans* and *D. gunungcola* body color
914 differences. (C) Multiplexed Shotgun Genotyping (MSG) (Andolfatto *et al*., 2011) was used to

915 estimate genome-wide ancestry assignments for a single introgression line generated by
916 repeatedly backcrossing *D. gunungcola* into a *D. elegans* genetic background (see Methods). The
917 posterior probability that a region is homozygous for *D. elegans* (red) or *D. gunungcola* (blue)
918 ancestry is plotted along the y-axis. (D) Representative wing spot images of *D. elegans* and *D.*
919 *gunungcola* species parents, the introgression line genotyped in (B), and an F_1 heterozygote
920 generated by crossing *D. elegans* females to introgression males. (E) Quantification of wing spot
921 size differences between each genotype. Results of Tukey HSD *post hoc* tests following one-way
922 ANOVA are shown (One-way ANOVA $F_{2,88} = 78.6$; $P < 2.0 \times 10^{-16}$; post-hoc Tukey HSD was
923 significant between *D. elegans* and Introgression: $P < 1.0 \times 10^{-7}$, *D. elegans* and F1
924 Inrogression/*D. elegans* heterozygote: $P = 0.02$, and Introgression and Inrogression/*D. elegans*
925 heterozygote: $P < 1.0 \times 10^{-7}$. Gray triangles represent individual replicates.
926
927
928
929
930 **Supplementary Figure S5 Fine-mapping the wing spot locus**
931
932 *D. elegans* and *D. gunungcola* backcross recombinants containing X chromosome breakpoints
933 immediately flanking the wing spot QTL peak were aligned to compare the effects of each on
934 wing pigmentation. Regions in red represent *D. elegans* linked loci, and regions in blue represent
935 *D. gunungcola* linked loci. All recombinants possessing *D. gunungcola* loci to the right of
936 ~10.95 Mbp are spotless.
937

Supplementary Figure S6 Effects of the *yellow* gene on wing spot size and wing display behavior in *D. elegans*

(A) Loss-of-function *D. elegans HK yellow* mutants develop smaller wing spots than *D. elegans HK* wild-type males (Student's t-test; t = 4.7759; df = 15.28; P = 0.0002; two-tailed) and (B) show lower maximum wing display angles (Student's t-test; t = 3.0294; df = 50.82; P = 0.004; two-tailed).

Supplementary Figure S7 Male wings from new *D. gunungcola* isolates

Male *D. gunungcola* from five newly collected isofemale lines in Indonesia do not develop wing spots.

Supplementary Figure S8 *In situ* hybridization of *D. elegans* and *D. gunungcola* pupal wings probed for *omb* mRNA

omb mRNA (purple) was probed at 30 and 48 h after pupal formation (APF) in both males and females.

Videos

Video 1 *D. elegans HK* wing display behavior

Video 2 *D. gunungcola SK* courtship and copulation

Video 3 F_1E wing display behavior

Video 4 F_1G wing display behavior

Video 5 Introgression 1 wing display behavior

Video 6 Introgression 2 wing display behavior

Video 7 Introgression 3 wing display behavior

Video 8 *D. gunungcola* wing display behavior at Coban Rondo Waterfall in East Java, Indonesia (Version 1)

Video 9 *D. gunungcola* wing display behavior at Coban Rondo Waterfall in East Java, Indonesia (Version 2)

Video 10 *D. elegans* wing display behavior in Tumpang, Indonesia

Video 11 *D. gunungcola* (Batu City, Indonesia) wing display behavior in the laboratory

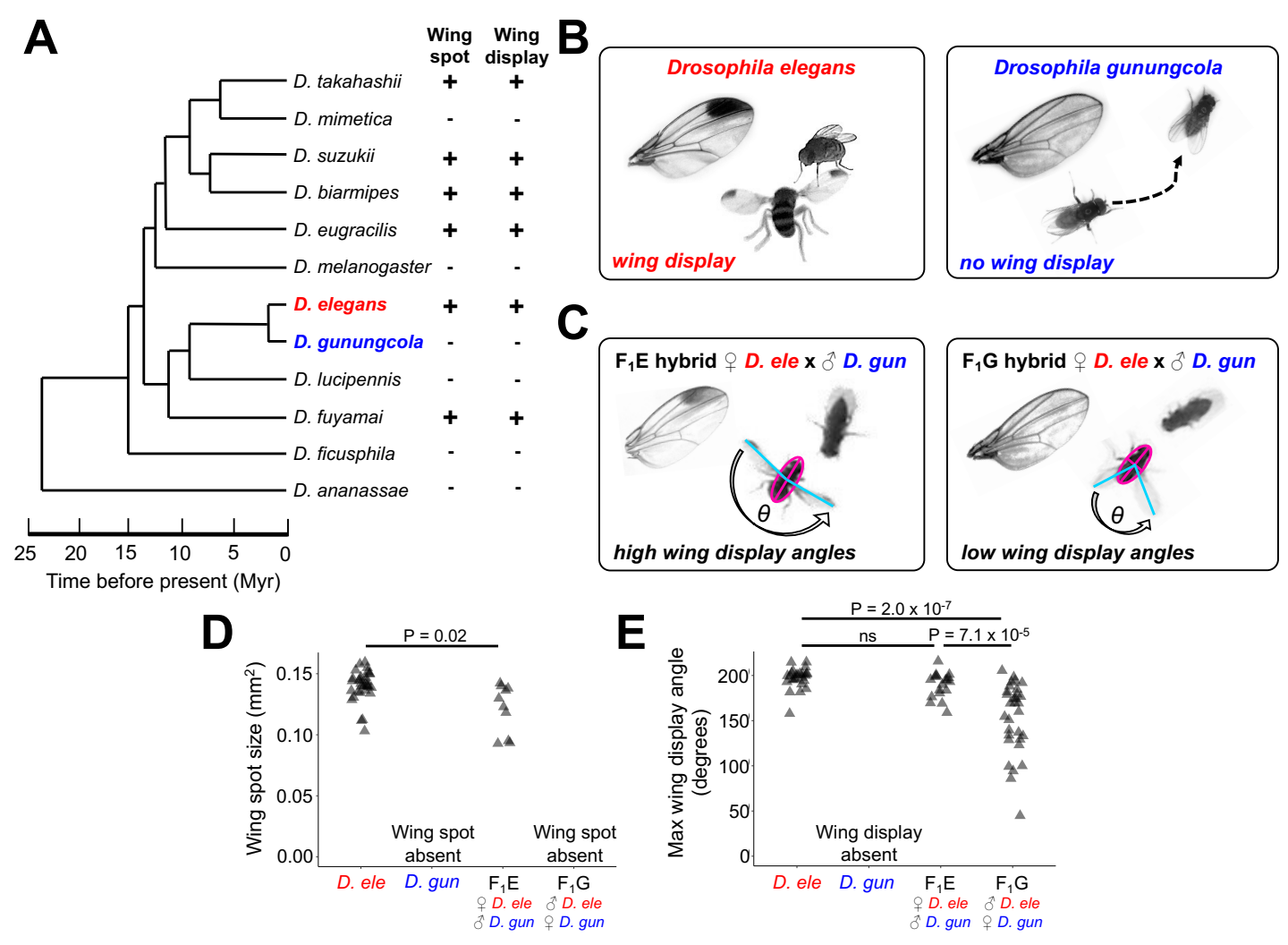
A
Wing spot
Wing display
D. takahashii + +
D. mimetica - -
D. suzukii + +
D. biarmipes + +
D. eugracilis + +
D. melanogaster - -
D. elegans + +
D. gunungcola - -
D. lucipennis - -
D. fuyamai + +
D. ficusphila - -
D. ananassae - -
25 20 15 10 5 0
Time before present (Myr)
B
Drosophila elegans
wing display
Drosophila gunungcola
no wing display
C
F1E hybrid ♀ D. ele x ♂ D. gun
high wing display angles
F1G hybrid ♀ D. ele x ♂ D. gun
low wing display angles
θ
D
P = 0.02
Wing spot size (mm2)
0.15
0.10
0.05
0.00
Wing spot absent
Wing spot absent
D. ele
D. gun
F1E
♀ D. ele
♂ D. gun
F1G
♂ D. ele
♀ D. gun
E
P = 2.0 x 10-7
ns
P = 7.1 x 10-5
Max wing display angle (degrees)
200
150
100
50
0
Wing display absent
D. ele
D. gun
F1E
♀ D. ele
♂ D. gun
F1G
♂ D. ele
♀ D. gun

A


width
length

B

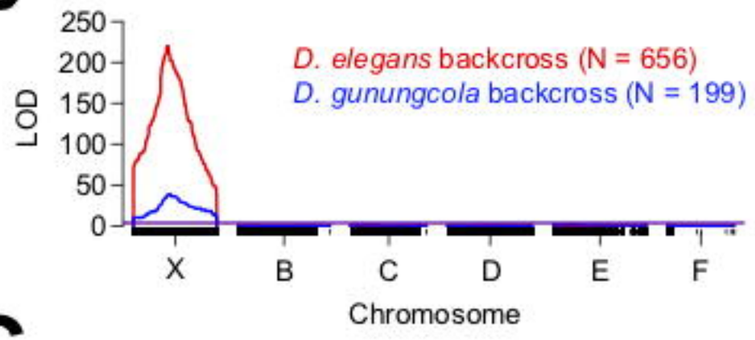
250
200
150
100
50
0
LOD
D. elegans backcross (N = 656)
D. gunungcola backcross (N = 199)
X
B
C
D
E
F
Chromosome

C

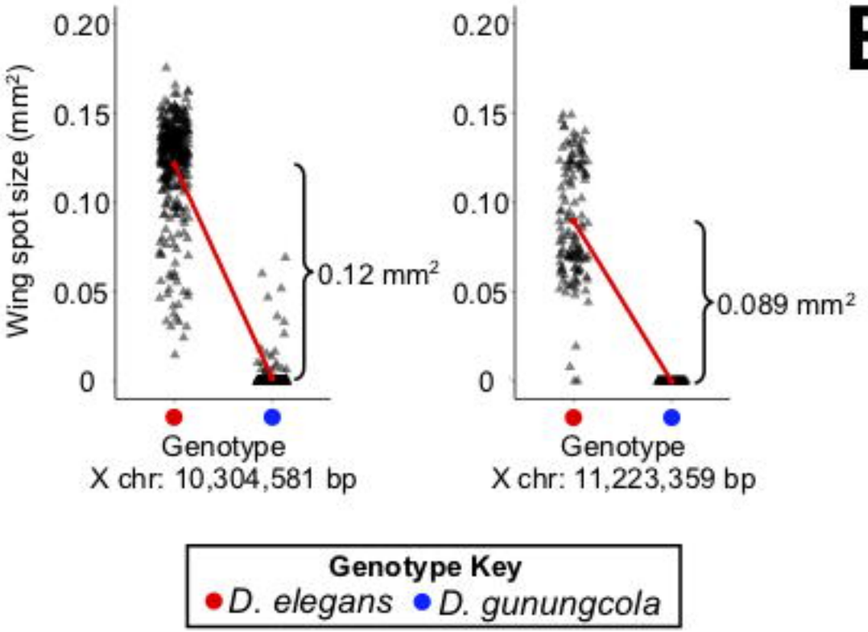
D. elegans backcross
D. gunungcola backcross
0.20
0.15
0.10
0.05
0
Wing spot size (mm²)
0.12 mm²
0.089 mm²
Genotype
X chr: 10,304,581 bp
Genotype
X chr: 11,223,359 bp
Genotype Key
D. elegans
D. gunungcola

D

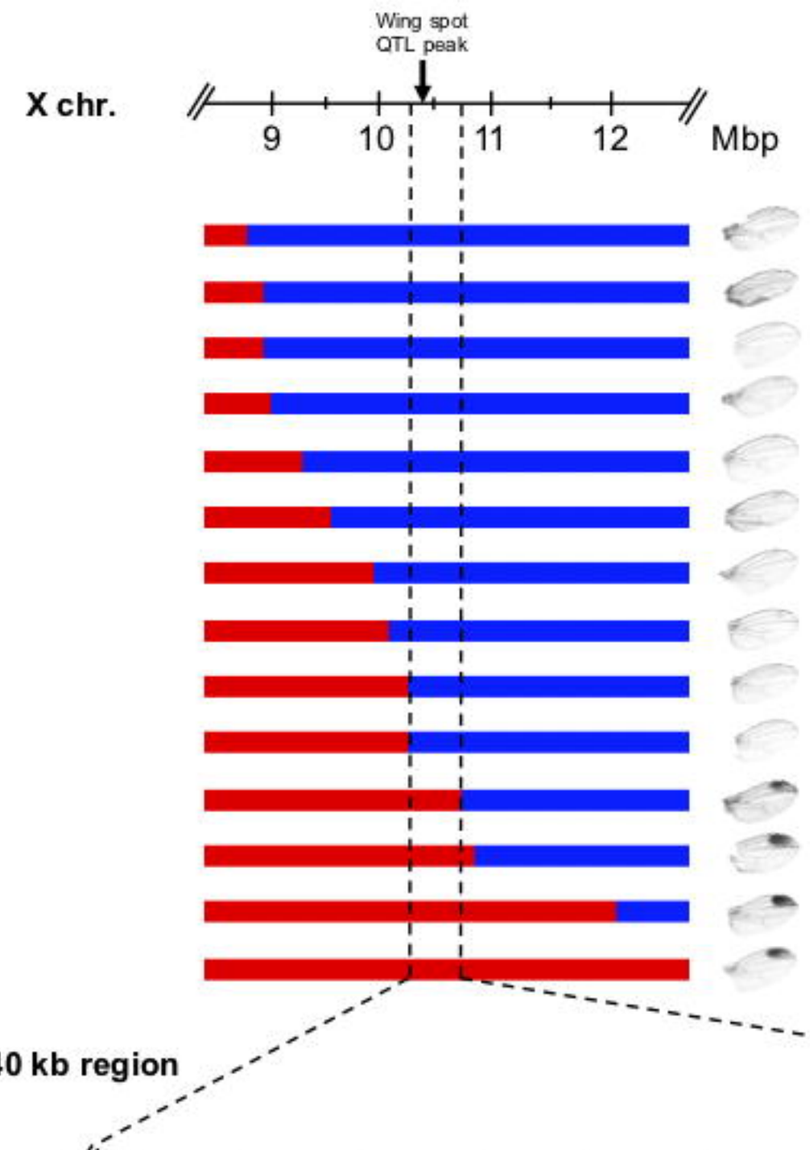
Wing spot
QTL peak
X chr.
9
10
11
12
Mbp

E

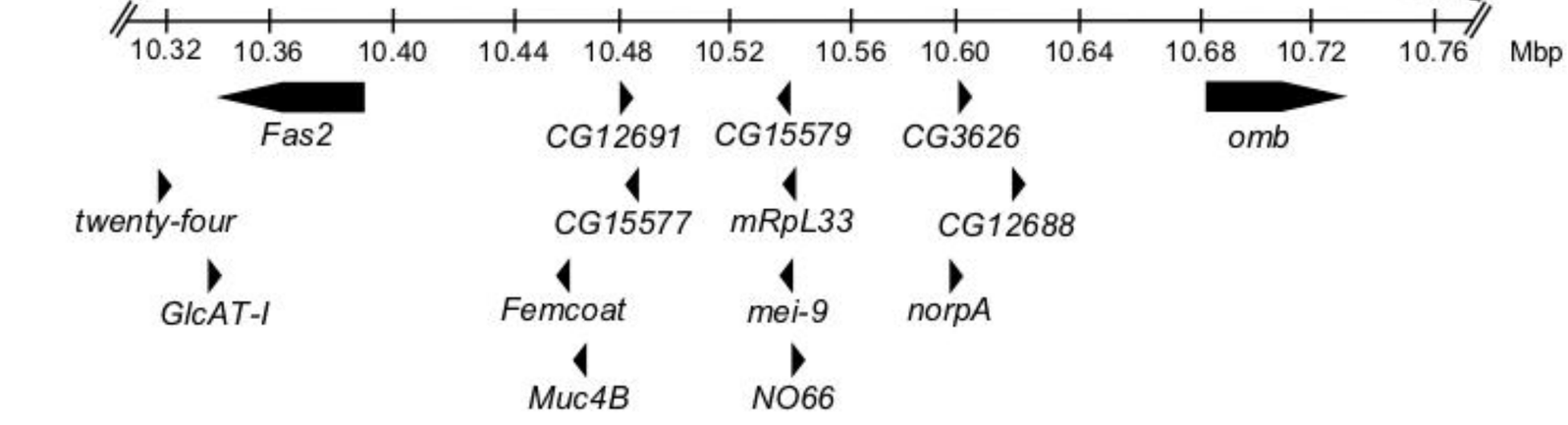
440 kb region
10.32
10.36
10.40
10.44
10.48
10.52
10.56
10.60
10.64
10.68
10.72
10.76
Mbp
Fas2
CG12691
CG15579
CG3626
omb
twenty-four
CG15577
mRpL33
CG12688
GlcAT-I
Femcoat
mei-9
norpA
Muc4B
NO66

F

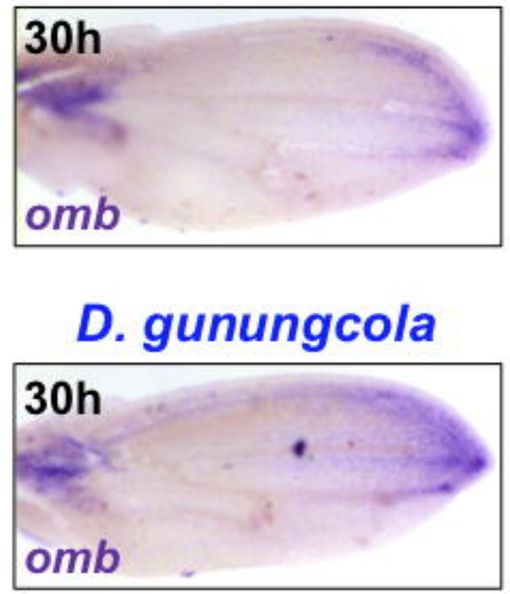
D. elegans
30h
omb
D. gunungcola
30h
omb

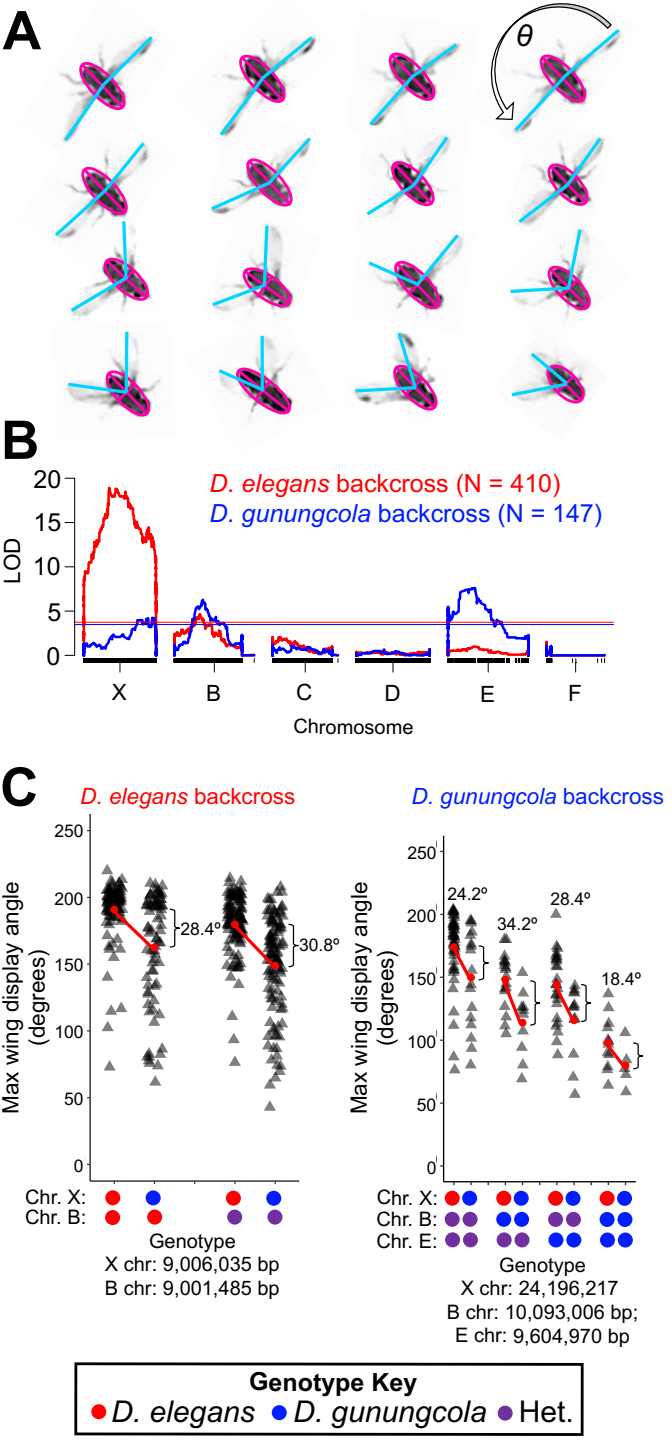
A
θ
B
D. elegans backcross (N = 410)
D. gunungcola backcross (N = 147)
LOD
20
15
10
5
0
X
B
C
D
E
F
Chromosome
C
D. elegans backcross
D. gunungcola backcross
Max wing display angle (degrees)
250
200
150
100
50
0
28.4°
30.8°
Chr. X:
Chr. B:
Genotype
X chr: 9,006,035 bp
B chr: 9,001,485 bp
24.2°
34.2°
28.4°
18.4°
Chr. X:
Chr. B:
Chr. E:
Genotype
X chr: 24,196,217
B chr: 10,093,006 bp;
E chr: 9,604,970 bp
Genotype Key
D. elegans
D. gunungcola
Het.

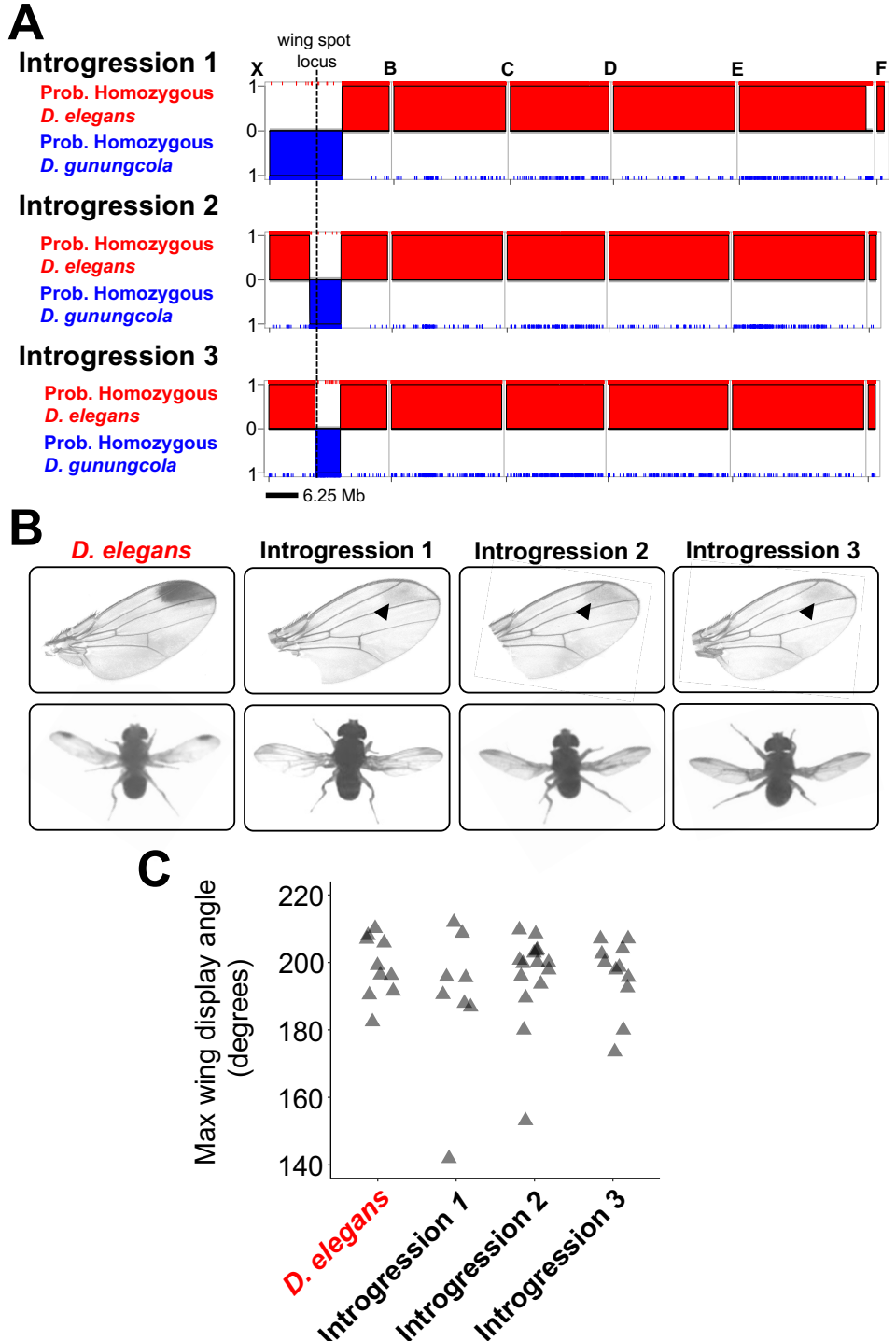
A
wing spot locus
X
B
C
D
E
F
Introgression 1
Prob. Homozygous D. elegans
Prob. Homozygous D. gunungcola
Introgression 2
Prob. Homozygous D. elegans
Prob. Homozygous D. gunungcola
Introgression 3
Prob. Homozygous D. elegans
Prob. Homozygous D. gunungcola
1
0
1
6.25 Mb
B
D. elegans
Introgression 1
Introgression 2
Introgression 3
C
Max wing display angle (degrees)
220
200
180
160
140
D. elegans
Introgression 1
Introgression 2
Introgression 3

Table 1 QTLs detected for wing spot size and maximum wing display angle divergence

Trait	Backcross	Chromosome	QTL interval (bp)[a]	QTL peak (bp)	LOD
Wing spot size	*D. elegans*	X	10,297,836-10,744,020	10,304,581	220
Max wing display angle	*D. elegans*	X	8,729,737-15,691,924	9,006,035	18.9
Max wing display angle	*D. elegans*	B	5,773,911-13,325,000	9,001,485	4.66
Wing spot size	*D. gunungcola*	X	10,474,499-11,584,862	11,223,359	38.9
Max wing display angle	*D. gunungcola*	X	16,885,658-25,539,528	24,196,217	4.23
Max wing display angle	*D. gunungcola*	B	7,078,659-12,180,268	10,093,006	6.28
Max wing display angle	*D. gunungcola*	E	3,813,413-11,535,144	9,604,970	7.59

[a] LOD drop 1.5 support interval